

SUPPORTING INFORMATION

High-transmittance and focal controllable plano-convex lenses with embedded nanolenses bottoms formed by electrowetting on a colloidal monolayer

Xiangmeng Li^{*ab}, Jinyou Shao^{*b}, Hongmiao Tian^b, Xiangming Li^b, Xiaoliang Chen^b, Xijing Zhu^a

^aShanxi Provincial Key Laboratory of Advanced Manufacturing Technology, North University of China, Taiyuan, Shanxi, 030051, China.

^bMicro- and Nano-technology Research Center, State Key Laboratory for Manufacturing Systems Engineering, Xi'an Jiaotong University, Xi'an, Shaanxi, 710049, China.

*Corresponding author: xmli123@nuc.edu.cn (Dr. Xiangmeng Li),

jyshao@mail.xjtu.edu.cn (Prof. Jinyou Shao)

Description for the list of figures and movies:

1. Experimental details

2. Supplementary figures and captions

Fig. S1. (a) Photograph illustration of the EWOD set-up for fabricating NOA72 lens on the contact angle measurement apparatus SCA20 (Dataphysics, GmbH, Germany). (b) The magnified picture of the real-time captured image on the screen during applying directional-current (DC) voltage of 100 V.

Fig. S2. The irreversibility of electrowetting of NOA72 droplet on the hydrophobic colloidal monolayer.

Fig. S3. Slow evolution of NOA72 droplets during applying voltage, indicating the possibility of ceasing at any state with a controlled contact angle.

Fig. S4. Photograph images of (a) NOA72 lenses obtained on the nanosphere monolayer and (b) NOA72 lenses transferred to the PET substrate. (c) NOA72 lens of varied sizes transferred onto the PET substrate, and (d) NOA72 lenses on a piece of white paper, indicating some scattering light due to sub-wavelength scale nanolens array.

Fig. S5. (a) Experimental set-up for measuring the light transmittance at the interface of NOA72 lens mounted onto an optical fiber probe, with light source of 532 nm laser (300 mW). Inset image shows the schematic illustration of the NOA72 lens mounted onto an optic probe. (b) Captured picture of the screen indicating the real-time measured light intensity (relative intensity, a.u.) from the spectrometer, which was normalized thereafter for varying incident angles.

Fig. S6. NOA72 lenses transferred to optical fiber for demonstration of focusing LED light, indicating (a) a smaller focus angle and (b) a smaller spots in comparison of that with and without the NOA72 lenses.

3. Supplementary videos

Movie S1: Electrowetting of a NOA72 droplet on the smooth flat fluoro-treated thermal-oxide silicon wafer surface by applying DC voltage of 200 V.

Movie S2: Electrowetting of a NOA72 droplet on the hydrophobic colloidal monolayer coating on thermal-oxide silicon wafer surface by applying DC voltage of 200 V.

1. Experimental details

1.1 Preparation of colloidal monolayer

Briefly, the colloidal monolayer of silica nanoparticles (SiNPs) was prepared using the method as reported by Yang et al¹. Firstly, a Si wafer with a 500 nm thick oxide layer was cleaned in a Piranha solution ($\text{H}_2\text{SO}_4:\text{H}_2\text{O}_2 = 3:1$ v%) at 95 °C in a water bath for 1 h, and washed thoroughly with deionized water, prior to baking on a 180 °C hotplate. Silica nanoparticles were synthesized using Stöber method². Then, colloidal film was prepared on the silicon wafer with Langmuir–Blodgett dip-coating method. An ethylene glycol solution of SiNPs (in diameter of 360 ± 20 nm) was supplied drop-wise on the water dish. A monolayer of SiNPs then spontaneously formed on the water–air interface because of the Marangoni effect. The Si wafer was then lifted up from the water by using a precise manipulator at a speed of $30\text{--}50 \mu\text{m s}^{-1}$. The floating SiNPs were gradually collected by the hydrophilic wafer. A close-packed colloidal film generated through self-assembly.

1.2 Preparation of hydrophobic colloidal monolayer

To enlarge the contact angle of both the aqueous solutions and polymeric droplet on the colloidal film, we should enhance the hydrophobicity of the monolayer as well as the silicon wafer. Accordingly, the colloidal film-coated sample was simply dipped in a glass of fluorosilane solution (mixture of F8063:F1061 = 100:1 v%) for 12 h, and heated at 150 °C oven for 3 h. Thus, the colloidal film became hydrophobic, with a water contact angle of 138°.

1.3 Experimental set-up for wetting properties characterization

We set up the observation platform on a professional contact angle measurement apparatus SCA20 (Dataphysics, GmbH, Germany). Plane white light was used as luminating source. The image and video of the droplet profile were taken by the charged coupled device (CCD). The colloidal coated sample was settled on the platform. Water droplet was supplied to the surface of the sample, and the static contact angles were measured before and after fluorine treatment. As for the dynamic contact angle measurement on the fluorine treated colloidal monolayer, we used a liquid supplier to supply and withdraw droplet, and recorded the advancing and receding contact angles with CCD camera.

1.4 Electrowetting observation

Electrowetting experiment was performed on the contact angle measurement apparatus SCA20. Then, a droplet of 2 μl NOA72 (Norland Optical adhesives, USA) on the nanoparticle monolayer (the volume of NOA72 droplet can be changed so as to obtain various size of lenses). A copper wire (with diameter of 100 or 200 μm) was adopted to apply voltage as an electrode by inserting into the NOA72 droplet, whereas a conductive tape was used as the other one electrode connected to the high-doped silicon wafer. By applying a direct-current (DC) voltage onto the liquid

droplet using a high-voltage DC power supplier (Keysight, USA), the shape of the NOA72 liquid lens would be changed with more contact area on the monolayer of SiNPs. The amplitude of the applying voltage was adjusted ranging from 0-600 V. The evolution of the electrowetting droplet could be observed on the screen, showing contact angle changing before and after applying voltage, as well as upon removal of the copper electrode. Finally, we could generate solidified NOA72 lenses by using UV-Ozone irradiation with 200 W of illumination power, for about 5 min.

1.5 Characterization of optical properties

The lens was peeled off with a pair of plastic tweezers, and transferred to the PET substrate for optical imaging. The imaging process was also performed on the OCA20 system, the patterns were recorded by the CCD. Lenses were also equipped onto one end of the optical fibre with diameter of 2 mm. With green LED illumination, we could observe the focal spot on the wall. In order to compare the light performance of NOA72 lenses with and without nanolens array, we measured the lens adhered to the PET substrate using a power meter, during a low-power laser was provided. The curvature radius R , focal length f , and numerical aperture NA , were calculated using formula as shown in literature³, given by

$$R = \frac{a^2 + h^2}{2h},$$

$$f = \frac{R}{n_s - 1},$$

$$NA = \frac{a}{f},$$

where a , h and R are the radius of base circle, sag height, and curvature radius of plano-convex lens, respectively, n_s is the refractive index of solidified NOA72.

Moreover, the incident angle dependent transmittance was measured using semiconductor lasers of two wavelengths, i.e., 808 nm and 532 nm (300 mW, Changchun Laser Optoelectronics Technology, China). An optic fiber probe and a power meter were adopted to measure the intensity of the extracting light at the plano-interfaces from NOA72 to the air. The incident angle was well tuned ranging from 0 to 80 degrees for both wavelengths of 532 nm and 808 nm. The intensity of measurement was normalized for the sake of comparison.

1.6 Morphological characterization for the lenses

Photograph of NOA72 lenses transferred onto a PET substrate was taken with digital camera, when they were arranged as letters "XJ" or other arrays. The morphologies of the obtained lens and the nanolens array structure on the flat surface of the NOA72 lenses were characterized in the field-emission scanning electron microscope (FE-SEM, SU-80, Hitachi, Japan), and laser confocal scanning microscope (LEXT 4000, Olympus, Japan).

1.7 Finite Differential Time Domain (FDTD) simulation

In this study, a three-dimensional (3D) model FDTD simulation was conducted using commercial software FDTD Solutions (Lumericals Solutions, Canada). The numerical work was done with a work station Z840 (HP, Hewlett-Packard Development Company). The size of FDTD simulation block was set as $2\ \mu\text{m} \times 2\ \mu\text{m} \times 2.5\ \mu\text{m}$. The air/polymer interface was set at the position of $-0.5\ \mu\text{m}$. The nanolens array was set as half embedded close-packed colloidal monolayer on the air/polymer interface. Planewave light sources was utilized. Monitor was set through the row center of nanolens array in the y - z plane. The light propagation through the simulation region was monitored and recorded. Finally, the light distribution of both the interface with and without nanolens array was compared.

To investigate the effect of the incident angle on the transmittance, 3D modelling of FDTD simulation was numerically studied to compare the transmittance at both the interfaces of NOA72 films with and without embedding nanolens array structures. The FDTD simulation size was set as $2.16\ \mu\text{m} \times 1.25\ \mu\text{m} \times 5.78\ \mu\text{m}$ in XYZ directions. Simulation time was set as 1000 fs, and the time step was about 0.018 fs. The boundary condition was set as BLOCH in X - Y orientations, while PML in Z orientation. Mesh size was set as $0.0094\ \mu\text{m}$ for the local region at the air/polymer interfaces. The refractive index was set as $n=1.56$ for the NOA72 region, while it was $n=1.45$ for the close-packed monolayer SiNPs (diameter of 360 nm) as half-embedded into the NOA72 region, and it was $n=1$ for the background region. Light sources was set as Plane wave with Bloch/Periodic type, and the wavelength was set as 532 nm and 808 nm, for both the nanolens array and flat bottoms. To obtain the angle dependence of the transmittance, the incident angle of light source was set as sweep parameters ranging from 0 to 80 degrees, with 10 degrees as an interval. The total time consumption of simulation was about 40 hours and 30 hours for nanolens-array and flat interfaces, respectively.

2. Supplementary figures and captions

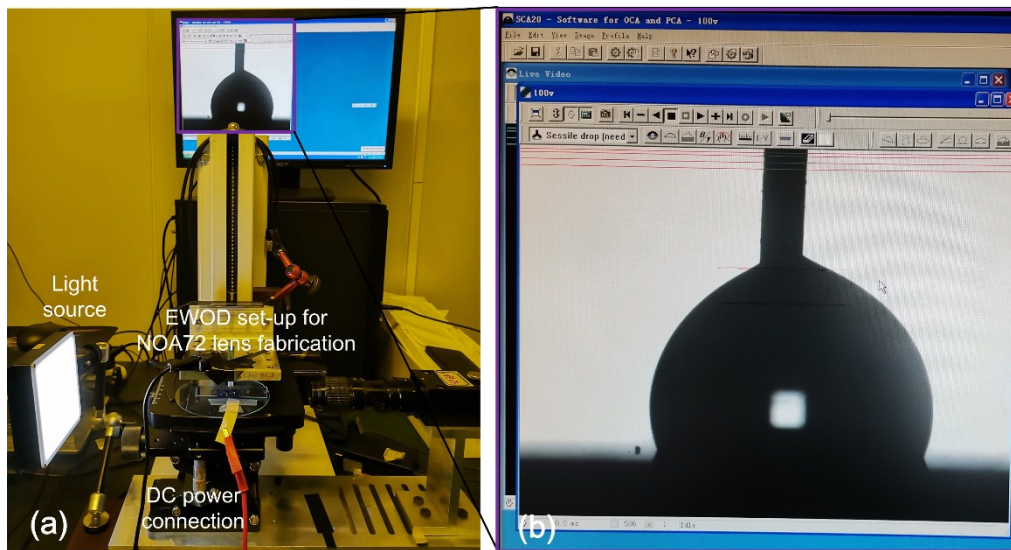


Fig. S1. (a) Photograph illustration of the EWOD set-up for fabricating NOA72 lens on the contact angle measurement apparatus SCA20 (Dataphysics, GmbH, Germany). (b) The magnified picture of the real-time captured image on the screen during applying directional-current (DC) voltage of 100 V.

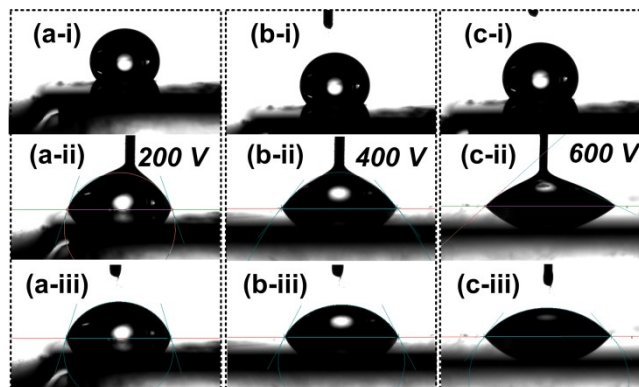


Fig. S2. The irreversibility of electrowetting of NOA72 droplet on the hydrophobic colloidal monolayer.

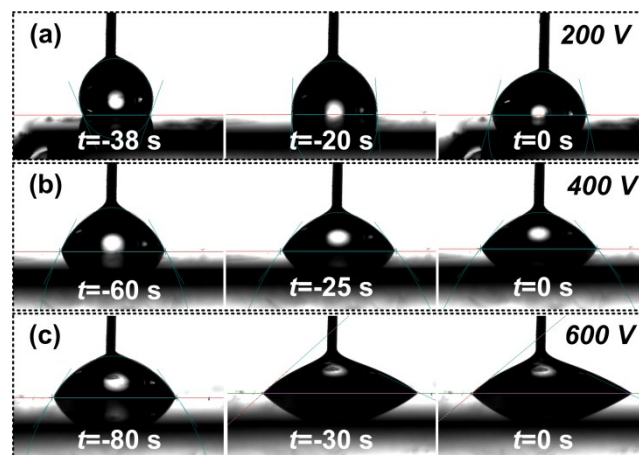


Fig. S3. Slow evolution of NOA72 droplets during applying voltage, indicating the possibility of ceasing at any state with a controlled contact angle.

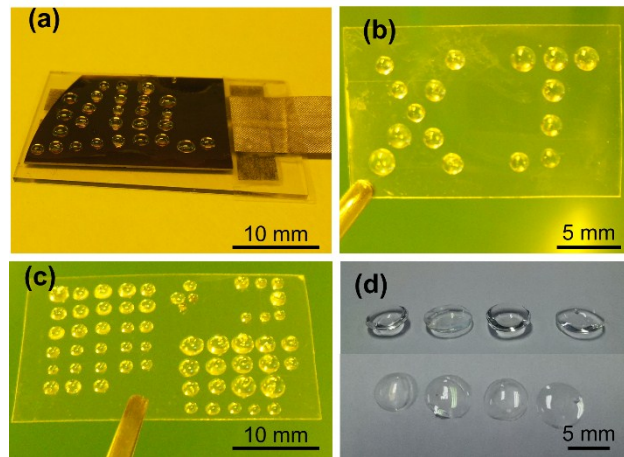


Fig. S4. Photograph images of (a) NOA72 lenses obtained on the nanosphere monolayer and (b) NOA72 lenses transferred to the PET substrate. (c) NOA72 lens of varied sizes transferred onto the PET substrate, and (d) NOA72 lenses on a piece of white paper, indicating some scattering light due to sub-wavelength scale nanolens array.

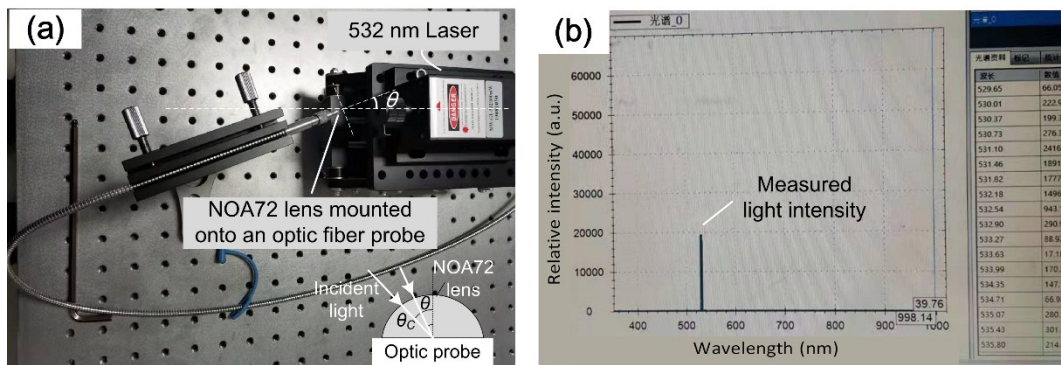


Fig. S5. (a) Experimental set-up for measuring the light transmittance at the interface of NOA72 lens mounted onto an optical fiber probe, with light source of 532 nm laser (300 mW). Inset image shows the schematic illustration of the NOA72 lens mounted onto an optic probe. (b) Captured picture of the screen indicating the real-time measured light intensity (relative intensity, a.u.) from the spectrometer, which was normalized thereafter for varying incident angles.

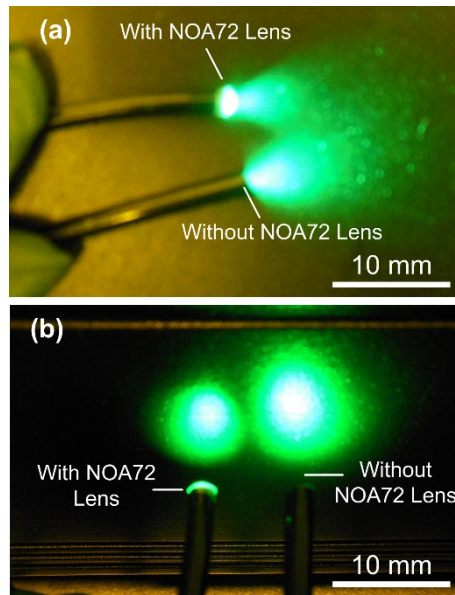


Fig. S6. NOA72 lenses transferred to optical fiber for demonstration of focusing LED light, indicating (a) a smaller focus angle and (b) a smaller spots in comparison of that with and without the NOA72 lenses.

References

1. H. Yang, B. Q. Li, X. Jiang, W. Yu and H. Liu, *Nanotechnology*, 2017, **28**, 505301.
2. W. F. STOBER, A; BOHN, E, *Journal of colloid and interface science*, 1968, **26**, 62.
3. Y. Luo, L. Wang, Y. Ding, H. Wei, X. Hao, D. Wang, Y. Dai and J. Shi, *Applied Surface Science*, 2013, **279**, 36-40.